NCT-Corrector: Non-Conformal Transformation Corrector for Convection-Dominated Boundary Layer Problems

MAS557 Theory and Application of Machine Learning
(Group 13) Dongseok Lee [1] Chanyoung Kim [1]

Abstract

This study explores the numerical approximation of two-dimensional convection-dominated singularly perturbed problems within a parametric domain. These types of boundary value problems pose significant challenges due to the presence of sharp boundary layers within their solutions. Traditional numerical methods often fail to effectively capture sharp singular layers, or they incur prohibitively high costs. Recently, various methods have been attempted, including those SL-PINN(G.-M. Gie & Munkhjin, 2024; T.-Y. Chang & Jung, 2024; G.-M. Gie & Jung, 2024), which have shown promise in addressing these issues. However, these methods are limited to orthogonal coordinate systems and primarily analyze conformal transformations. We introduce a Non-Conformal Transformation Corrector, NCT-Corrector incorporated with SL-PINN methodology for broader analysis. The NCT-PINN method effectively predicts solutions for problems with sharp transitions in complex domains that are difficult for conventional methods to handle.

1. Introduction

The use of neural networks for approximating solutions to differential equations has gained significant attention in research (Jin et al., 2021).

Various unsupervised neural network methods have been developed within this domain, including physics-informed neural networks (PINNs) (Lu et al., 2021), the deep Ritz method (DRM) (Yu et al., 2018), and the Galerkin Neural Network (GNN) (Ainsworth & Dong, 2022).

PINNs, in particular, utilize collocation points in the space-time domain as inputs, making them well-suited for solving complex, time-dependent, multi-dimensional equations with intricate domain geometries. However, PINNs exhibit limitations in accurately capturing complex and highly nonlinear flow patterns such as turbulence, vortical structures, and boundary layers (Fernández de la Mata et al., 2023; Bararnia & Esmaeilpour, 2022; Gomes et al., 2022; Han & Lee, 2023).

In this paper, we introduce the boundary layer problem, which poses a significant challenge for PINNs. We propose a method to resolve this issue by enhancing performance through the incorporation of a semi-analytic approach into the PINN framework.

Our focus is on two-dimensional convection-diffusion equations in parametric regions denoted by Ω:

$$\begin{aligned} L_\epsilon u^\epsilon := -\epsilon \Delta u^\epsilon - u^\epsilon_y = f, \quad & \text{in } \Omega, \\ u^\epsilon = 0, \quad & \text{at } \partial\Omega. \end{aligned}$$

We construct a two-layer neural network similar to PINNs, emphasizing hard constraints for boundary conditions:

$$\overline{u}(x, y; \boldsymbol{\theta}) = g(x, y)\hat{u}(x, y; \boldsymbol{\theta}),$$

where $\hat{u}$ is defined by a two-layer neural network, with $g(x, y) = 0$ on $\partial\Omega$:

$$\hat{u}(x, y; \boldsymbol{\theta}) = \sum_{j=1}^{n} c_j \sigma(w_{1j}x + w_{2j}y + b_j),$$

using logistic sigmoid activation $\sigma(z) = \frac{1}{1+e^{-z}}$. This simplified structure allows calculating the loss function using explicit derivatives of $\hat{u}$, avoiding computational errors with boundary layers. Our approach is cost-effective and accurate, with potential extension to multi-layer networks using symbolic computation. While traditional PINNs use multi-layer architectures, our SL-PINNs use a two-layer structure but achieve superior performance.

[1]Department of Mathematics, Korea Advanced Institute of Science and Technologies, Daejeon, Korea. Correspondence to: Youngjoon Hong <hongyj@kaist.ac.kr>.

MAS557 Final Project, 2024.

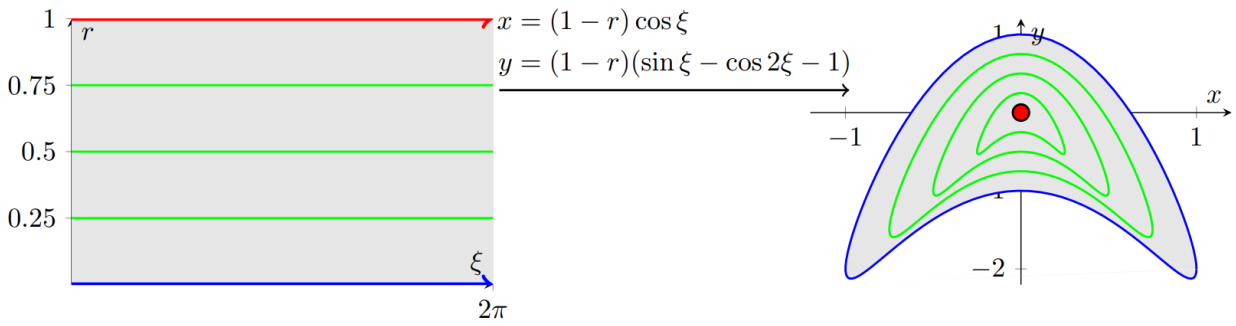

Figure 1. The boundary-fitted coordinates D^* (left) and the parametric region D (right) with the generalized coordinate transformations without orthogonal coordinate system.

2. Boundary Layer Analysis

2.1. Parametrization

Our aim in this article is to study singularly perturbed problems of the form

$$\begin{cases} L_\varepsilon u^\varepsilon := -\varepsilon \Delta u^\varepsilon - u^\varepsilon_y = f(x,y) \text{ in } D, \\ u^\varepsilon = 0 \text{ on } \partial D, \end{cases} \tag{1}$$

where $0 < \varepsilon \ll 1$.
We denote the upper and lower halves of the domain by $C_u(x) = \sqrt{1-x^2} - 2x^2$. The limit problem (i.e., when $\varepsilon = 0$) is defined by

$$\begin{cases} -u^0_y = f(x,y) \text{ in } D, \\ u^0 = 0 \text{ on } \Gamma_u, \end{cases} \tag{2}$$

where $\Gamma_u = \{(x,y) \mid x^2 + y^2 = 1, y > 0\}$. The explicit solution of equation (2) is

$$u^0(x,y) = \int_y^{C_u(x)} f(x,s)ds, \quad (x,y) \in D. \tag{3}$$

Before proceeding, we introduce the formal asymptotic expansion of u^ε, $u^\varepsilon \sim \sum_{j=0}^{\infty} \varepsilon^j u^j$, also known as the outer expansion in boundary layer theory. This expansion leads to

$$\begin{cases} -u^j_y = \Delta u^{j-1} & \text{in } D, \\ u^j = 0 & \text{on } \Gamma_u. \end{cases} \tag{4}$$

In our analysis, we assume that the following conditions hold:

$$\frac{\partial^{p_1+p_2} f}{\partial x^{p_1} \partial y^{p_2}} = 0 \text{ at } (\pm 1, -2) \text{ for } 0 \le 2p_1 + p_2 \le 2 + 3n, \tag{5}$$

for $p_1, p_2 \ge 0$.For experiments and examples, the second compatibility condition, as listed below, was used:

$$\frac{\partial^{p_1+p_2} f}{\partial x^{p_1} \partial y^{p_2}} = 0 \quad \text{at} \quad (\pm 1, -2) \text{for} \quad 0 \le 2p_1 + p_2 \le 2. \tag{6}$$

2.2. Non-Conformal Corrector

We introduce a non-conformal corrector θ^0 to adjust boundary values at critical points, deriving equations and establishing solutions using analytical and numerical methods. Full error analysis and further lemmas ensure the robustness of our results, aiming to approximate solutions efficiently and accurately. Considering the stretched variable $\tilde{r} = \frac{r}{\epsilon}$ we identify the dominating differential operators and we are led to the following equation for the first corrector θ^0:

$$\begin{cases} \dfrac{\partial^2 \theta^0}{\partial \tilde{r}^2} + \dfrac{H'}{S}(\xi) \sin \xi \dfrac{\partial \theta^0}{\partial \tilde{r}} = 0 \\ \text{for } 0 < \tilde{r} < \infty, \pi < \xi < 2\pi, \\ \theta^0 = -u^0(\cos\xi, (\sin\xi - \cos 2\xi - 1)) \\ \text{at } \tilde{r} = 0, \\ \theta^0 \to 0 \quad \text{as } \tilde{r} \to \infty. \end{cases} \tag{7}$$

Hence we are able to obtain an explicit solution:

$$\theta^0 = -u^0(\cos\xi, (\sin\xi - \cos 2\xi - 1)) \exp\left(\frac{\mathcal{W} \sin\xi r}{\epsilon}\right) \chi_{[\pi,2\pi)}(\xi), \tag{8}$$

We define χ_A as the characteristic function of the set A. Additionally, let

$$\mathcal{W} = -\frac{H'}{S},$$

where H' and S are previously defined functions, and $\mathcal{W}$ belongs to $C^\infty([0, 2\pi])$.

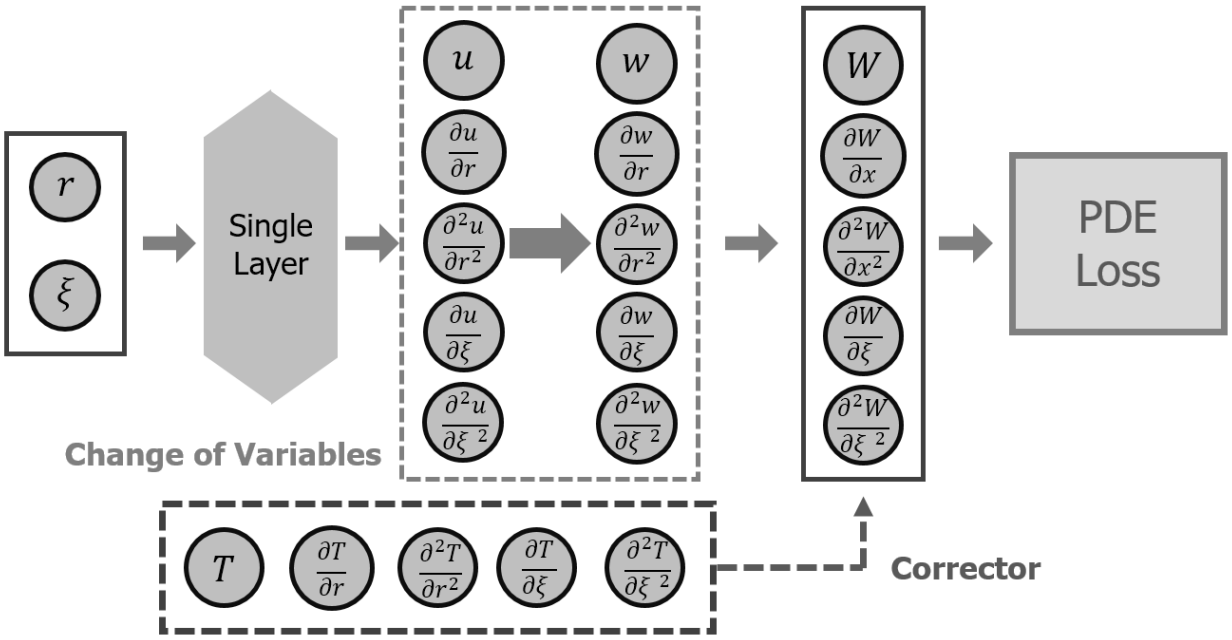

Figure 2. Schematic diagram of SL-PINN structure. The model utilize only a single layer consisting of trainable parameters. The training objective is incorporated by a single-layer prediction and the correction scheme with appropriate changes of variables.

Using a cut-off function we write an approximate form of θ^0:

$$\bar{\theta}^0 = -u^0(x(\xi), y(\xi)) \exp\left(\frac{\mathcal{W}\sin\xi r}{\epsilon}\right)\delta(r)\chi_{[0,\pi)}(\xi), \tag{9}$$

where $\delta(r)$ is a smooth cut-off function such that $\delta(r) = 1$ for $\xi \in [0, R/4]$ and $= 0$ for $\xi \in [R/2, R]$.

we simply use

$$B_x(\xi) = \cos\xi \tag{10}$$

$$B_y(\xi) = \sin\xi - \cos 2\xi - 1 \tag{11}$$

$$\bar{\theta}^0 = -u^0(B_x(\xi), B_y(\xi)) \exp\left(\frac{\mathcal{W}\sin\xi r}{\epsilon}\right)\delta(r)\chi_{[0,\pi)}(\xi), \tag{12}$$

Since θ^0 vanishes like u^0 at $\xi = \pi, 2\pi$, θ^0 is continuous and piecewise smooth on $\overline{D}$, and thus we conclude that $\theta^0, \bar{\theta}^0 \in H^1(D)$. We note here that

$$u^0(B_x(\xi), B_y(\xi)) = \int_{B_y(\xi)}^{B_y(-\xi)} f(B_x(\xi), s)\, ds, \quad \text{for} \quad \pi < \xi < 2\pi.$$

and

$$u^0 + \theta^0 \in H_0^1(D). \tag{13}$$

3. SL-PINN

To accurately capture the sharp, thin transition at the boundary layer, a naive PINN with 5 or 6 layers is insufficient. However, by incorporating the Corrector method, a single-layer PINN (SL-PINN) can achieve high accuracy in capturing this thin layer.

We make use of a straightforward neural network, $\hat{u}$, multiplied by $g(r, \xi)$ to satisfy the boundary condition as follows:

$$\hat{v}(r, \xi;\, \boldsymbol{\theta}) = g(r, \xi)\, \hat{u}(r, \xi;\, \boldsymbol{\theta}),$$

where $\hat{u}$ is defined by a two-layer neural network, with $g(r, \xi) = 0$ on Γ_u.

We define the two-layer neural network as:

$$\hat{u}(r, \xi;\, \boldsymbol{\theta}) = \sum_{j=1}^{n} c_j \sigma(w_{1j} r + w_{2j}\xi + b_j),$$

where n is the number of neurons.

We now establish the semi-analytic SL-PINN method as follows:

$$\widetilde{v}(r, \xi;\, \boldsymbol{\theta}) = (\hat{v}(r, \xi;\, \boldsymbol{\theta}) - \hat{v}(1, \xi;\, \boldsymbol{\theta})\bar{\varphi}^0)C(r, \xi),$$

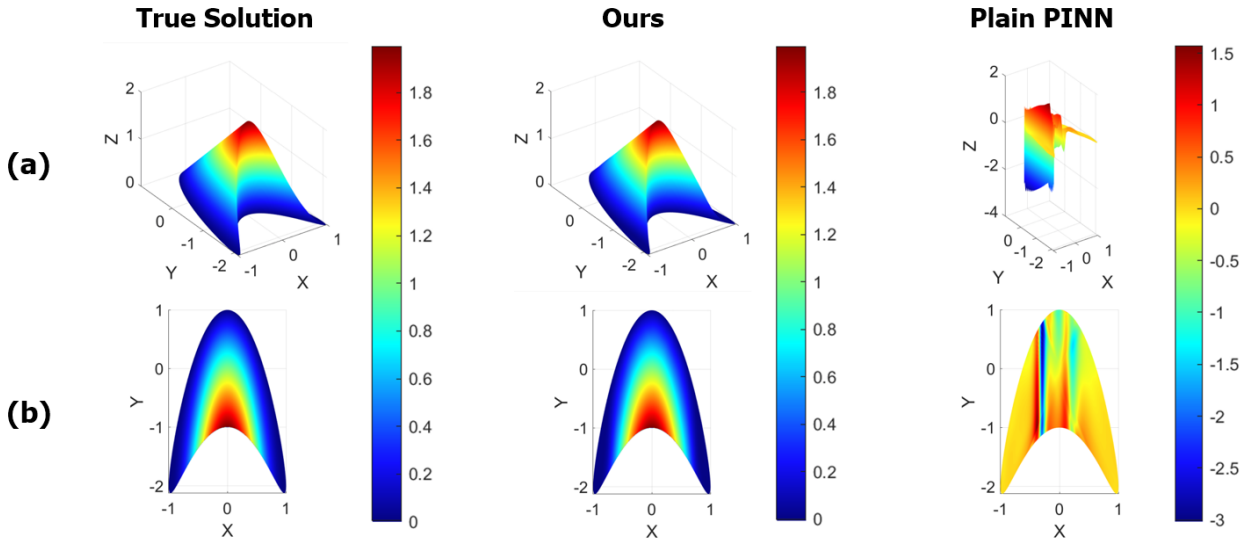

Figure 3. The true solution profile, along with the predictions of the SL-PINN approach and the naive PINN, are presented in both a 3D view (a) and a top-down view (b). This illustrates the profiles viewed from a three-dimensional perspective in (a) and from above in (b).

where $C(r, \xi)$ is given by

$$C(r,\xi) = \begin{cases} 1 - r^3, \text{ if } 0 \le \xi \le \pi, \\ 1 - r^3 - (r\sin\xi)^3, \text{ if } \pi < \xi < 2\pi, \end{cases} \tag{14}$$

4. Results

On the solid ground of the analysis, we conducted experiments to demonstrate the capability of our SL-PINN to detect the dramatic stiffness on the generalized parametric region. For the experiment, we utilize a single layer with 320 trainable parameters in the SL-PINN structure. The plain PINN model has 3360 trainable parameters, which is 10 times more than our approach. We trained both models for 500 epoch, and compared the predictive performance of both models against the ground truth. We employed the relative L2 norm and relative L-infinite norm as comparative metrics to assess the disparity between the two models, as these measures are well-suited for evaluating differences in function.

$$\text{Relative } L_2 \text{ norm} = \frac{\sqrt{\int_D (f(x) - g(x))^2 \, dx}}{\sqrt{\int_D f(x)^2 \, dx}}$$

$$\text{Relative } L_\infty \text{ norm} = \frac{\sup_{x \in D} |f(x) - g(x)|}{\sup_{x \in D} |f(x)|}$$

In the experiment, as shown in Figure 3, the two models exhibited a stark contrast, with our model demonstrating a proficient prediction of the solution's stiffness in the boundary layer. On the contrary, the plain PINN failed to capture the stiffness at the boundary layer, attributed to the absence of a complementary function that regulates abrupt stiffness at the boundary

Table 1. Comparison table of our model and naive PINN using relative L_2 norm and relative L_∞

MODELS	*Relative* L_2 *norm*	*Relative* L_∞ *norm*
OURS	**0.024**	**0.054**
Plain PINN	1.143	1.884

Conclusion

In this study, we present a semi-analytic method to improve the numerical performance of Physics-Informed Neural Networks (PINNs) in solving various singularly perturbed boundary value problems and convection-dominated equations on parametric domains. For each examined singular perturbation problem, we derive an analytic approximation, called the corrector function, which captures the behavior of the fast (stiff) component of the solution within the boundary layer. By integrating these corrector functions into a 2-layer PINN framework, we effectively manage the stiffness in the approximate solutions, resulting in our semi-analytic SL-PINNs enhanced with correctors. This incorporation of corrector functions allows us to address the stiffness challenge in approximate solutions, leading to the development

of improved SL-PINNs.

References

Ainsworth, M. and Dong, J. Galerkin neural network approximation of singularly-perturbed elliptic systems. *Computer Methods in Applied Mechanics and Engineering*, pp. 115169, 2022.

Bararnia, H. and Esmaeilpour, M. On the application of physics informed neural networks (pinn) to solve boundary layer thermal-fluid problems. *International Communications in Heat and Mass Transfer*, 132:105890, 2022. ISSN 0735-1933. doi: https://doi.org/10.1016/j.icheatmasstransfer.2022.105890. URL https://www.sciencedirect.com/science/article/pii/S0735193322000124.

Fernández de la Mata, F., Gijón, A., Molina-Solana, M., and Gómez-Romero, J. Physics-informed neural networks for data-driven simulation: Advantages, limitations, and opportunities. *Physica A: Statistical Mechanics and its Applications*, 610:128415, 2023. ISSN 0378-4371. doi: https://doi.org/10.1016/j.physa.2022.128415. URL https://www.sciencedirect.com/science/article/pii/S0378437122009736.

G.-M. Gie, Y. Hong, C.-Y. J. and Munkhjin, T. Semi-analytic pinn methods for boundary layer problems in a rectangular domain. *Journal of Computational and Applied Mathematics*, 2024.

G.-M. Gie, Y. H. and Jung, C.-Y. Semi-analytic pinn methods for singularly perturbed boundary value problems. *Applicable Analysis*, 2024.

Gomes, A. T. A., da Silva, L. M., and Valentin, F. Physics-aware neural networks for boundary layer linear problems, 2022.

Han, J. and Lee, Y. A neural network approach for homogenization of multiscale problems. *Multiscale Modeling & Simulation*, 21(2):716–734, 2023. doi: 10.1137/22M1500903. URL https://doi.org/10.1137/22M1500903.

Jin, X., Cai, S., Li, H., and Karniadakis, G. E. Nsfnets (navier-stokes flow nets): Physics-informed neural networks for the incompressible navier-stokes equations. *Journal of Computational Physics*, 426:109951, 2021.

Jung, C.-Y. and Temam, R. Convection–diffusion equations in a circle: The compatible case. *Journal de Mathématiques Pures et Appliquées*, 96(1):88–107, 2011. ISSN 0021-7824. doi: https://doi.org/10.1016/j.matpur.2011.03.006.

Lu, L., Meng, X., Mao, Z., and Karniadakis, G. E. Deepxde: A deep learning library for solving differential equations. *SIAM Review*, 63(1):208–228, 2021.

T.-Y. Chang, G.-M. Gie, Y. H. and Jung, C.-Y. Singular layer physics informed neural network method for plane parallel flows. *Computers and Mathematics with Applications*, 2024.

Yu, B. et al. The deep ritz method: a deep learning-based numerical algorithm for solving variational problems. *Communications in Mathematics and Statistics*, 6(1):1–12, 2018.

A. Lemma

We assume that

$$\frac{\partial^{\alpha+\beta} f(x,y)}{\partial x^{\alpha}\partial y^{\beta}} = 0 \quad \text{at } (\pm 1,-2), \quad 0 \le 2\alpha+\beta \le \gamma-1, \quad \gamma \ge 1, \quad \alpha,\beta \ge 0, \tag{15}$$

where $f(x,y)$ belongs to $C^{\gamma}(D)$, and D is the ellipse as in (1). Then the following function

$$\frac{f(x,C_u(x))}{(C_0(x))^{\gamma}} \tag{16}$$

is bounded for all $x \in (-1,1)$, where $C_0(x) = \sqrt{1-x^2}$.

Proof.

It suffices to show that $\frac{f(x,C_u(x))}{C_0^{\gamma}(x)}$ is bounded (has a finite limit) as $x \to 1^-$, -1^+. Since the case $x = -1^+$ is similar, we just consider the limit as $x \to 1^-$. To prove that $\lim_{x\to 1^-} \frac{f(x,C_u(x))}{C_0^{\gamma}(x)}$ is bounded, we proceed by induction on m, and use L'Hôpital's rule and the fact that $C_0'(x) = -xC_0^{-1}(x)$. For $m = 1$, we just observe that

$$\lim_{x\to 1^-} \frac{f(x,C_u(x))}{C_0(x)} = \lim_{x\to 1^-} \frac{f_x(x,C_u(x)) + f_y(x,C_u(x))(C_0'(x)-4x)}{C_0'(x)} = \lim_{x\to 1^-} f_y(x,C_u(x))$$

Assuming that the result holds for $y \le k$, $k \ge 1$, we then verify the claim for $y = k+1$ observing that

$$\lim_{x\to 1^-} \frac{f(x,C_u(x))}{C_0^{k+1}(x)} = -\lim_{x\to 1^-} \left(\frac{f_x(x,C_u(x))}{(k+1)xC_0^{k-1}(x)} + \frac{f_y(x,C_u(x))}{(k+1)C_0^{k}(x)} + \frac{4f_y(x,C_u(x))}{(k+1)C_0^{k-1}(x)} \right)$$

Since y is replaced by $k+1$, we are assuming that f belongs to $C^k(D)$ and satisfies 2.7 for $0 \le 2\alpha+\beta \le k-1$ and g_x belongs to $C^k(D)$ and satisfies 2.7 for $0 \le 2\alpha+\beta \le k-2$. It follows from the induction assumption that each of the terms in the right-hand side of 2.10 has a finite limit as $x \to 1^-$, and thus so does the term in the left-hand side. The lemma is proved.

B. Lemma

There exists a positive constant k such that, for integers $l, n, s \ge 0$, $m = 0,1,2$, and for $1 \le p \le \infty$,

$$\left| (\sin\xi)^{-l} \left(\frac{r}{\varepsilon}\right)^{n} \frac{\partial^{s+m}\theta^0}{\partial r^s \partial \xi^m} \right|_{L_p(D^*)} \le k \sup_{\xi} |a_{0,h}(\xi)| \varepsilon^{\frac{1}{p}-s}, \tag{17}$$

where $h = -s+m+l+n+1$, and

$$a_{0,q}(\xi) = \sum_{\substack{m+h+r\le q \\ m,h,r\ge 0}} c_{m,h,r} \frac{1}{\mathcal{W}^h \sin^m \xi} \frac{d^r v^0(\xi)}{d\xi^r}, \tag{18}$$

$v^0(\xi) = -u^0(B_x(\xi), B_y(\xi))$ and the $c_{m,r} = c_{m,r}(\xi) \in C^{\infty}([0,2\pi])$, may be different at different occurrences, If $q < 0$, then $a_{0,q}$ is simply in $C^{\infty}([0,2\pi])$ fuction. The notation $a_{0,q}$ follows the same convention as outlined in the *Notation convection* of (Jung & Temam, 2011).

Proof.

For integers $s \ge 0, m = 0,1,2$, we obtain

$$\frac{\partial^{s+m}\theta_0}{\partial \bar{r}^s \partial \xi^m} = \epsilon^s \frac{\partial^{s+m}\theta_0}{\partial r^s \partial \xi^m} = a_{0,-s+m}(\xi) \sum_{k=0}^{m} \left((-\mathcal{W}\sin\xi)\bar{r}\right)^k \exp\left((\mathcal{W}\sin\xi)\bar{r}\right) \chi_{[\pi,2\pi]}(\xi) \tag{19}$$

Hence, we observe that

$$(\sin\xi)^{-l}\bar{r}^n\frac{\partial^{s+m}\theta_0}{\partial r^s\partial\xi^m}=a_{0,-s+m}(\xi)(\sin\xi)^{-1-l-n}\sum_{k=0}^{m}(-\sin\xi)\left((-\mathcal{W}\sin\xi)\bar{r}\right)^{k+n}\epsilon^{-s}\exp\left((\mathcal{W}\sin\xi)\bar{r}\right)\chi_{[\pi,2\pi]}(\xi), \quad (20)$$

$$\left|(\sin\xi)^{-l}\bar{r}^n\frac{\partial^{s+m}\theta_0}{\partial r^s\partial\xi^m}\right|_{L^p(D^*)} \quad (21)$$

$$=\left|a_{0,-s+m}(\xi)(\sin\xi)^{-1-l-n}\sum_{k=0}^{m}(-\sin\xi)\left((-\mathcal{W}\sin\xi)\bar{r}\right)^{k+n}\epsilon^{-s}\exp\left((\mathcal{W}\sin\xi)\bar{r}\right)\right|_{L^p((0,R)\times(\pi,2\pi))} \quad (22)$$

$$\leq k\left\{\sup_{\xi}|a_{0,-s+m+l+n+1}(\xi)|\right\}\left(\int_{\pi}^{2\pi}\int_{0}^{1}|\sum_{k=0}^{m}\left((-\mathcal{W}\sin\xi)\bar{r}\right)^{k+n}|^p(-\sin\xi)^p\epsilon^{-ps}\exp\left((p\mathcal{W}\sin\xi)\bar{r}\right)drd\xi\right)^{\frac{1}{p}} \quad (23)$$

$$\leq k\left\{\sup_{\xi}|a_{0,-s+m+l+n+1}(\xi)|\right\}\left(\int_{\pi}^{2\pi}\int_{0}^{1}\kappa(-\sin\xi)^p\epsilon^{-ps}\exp\left((p\mathcal{W}\sin\xi)\bar{r}\right)drd\xi\right)^{\frac{1}{p}} \quad (24)$$

Note that

$$0\leq\int_0^1\exp\left(c\mathcal{W}(\sin\xi)\bar{r}\right)dr=\int_0^1\exp\left(c\mathcal{W}(\xi)(\sin\xi)\frac{r}{\epsilon}\right)dr=\frac{\epsilon}{-c\mathcal{W}(\xi)\sin\xi}\left[1-\exp\left(\frac{c\mathcal{W}\sin\xi}{\epsilon}\right)\right]. \quad (25)$$

Since $c\mathcal{W}(\xi)\sin\xi\leq 0$,

$$0\leq\int_0^1\exp\left(c(\mathcal{W}\sin\xi)\bar{r}\right)dr\leq\frac{\epsilon}{-c\mathcal{W}\sin\xi}, \quad (26)$$

Therefore,

$$0\leq\int_{\pi}^{2\pi}\int_0^1(-\sin\xi)^p\exp\left(c(\mathcal{W}\sin\xi)\bar{r}\right)drd\xi\leq\int_{\pi}^{2\pi}(-\sin\xi)^p\int_0^1\exp\left(c(\mathcal{W}\sin\xi)\bar{r}\right)drd\xi \quad (27)$$

$$\leq\int_{\pi}^{2\pi}(-\sin\xi)^p\frac{\epsilon}{-c\mathcal{W}\sin\xi}d\xi\leq\int_{\pi}^{2\pi}(-\sin\xi)^{p-1}\frac{\epsilon}{c\mathcal{W}}d\xi, \quad (28)$$

With $\kappa:=\int_{\pi}^{2\pi}(-\sin\xi)^{p-1}\frac{1}{c\mathcal{W}}d\xi$,

$$\int_{\pi}^{2\pi}\int_0^1(-\sin\xi)^p\exp\left(c(\mathcal{W}\sin\xi)\bar{r}\right)drd\xi\leq\kappa\epsilon. \quad (29)$$

Then, we obtain

$$\left|(\sin\xi)^{-l}\left(\frac{r}{\varepsilon}\right)^n\frac{\partial^{s+m}\theta^0}{\partial r^s\partial\xi^m}\right|_{L_p(\Omega^*)}\leq\kappa\sup_{\xi}|a_{0,-s+m+l+n+1}(\xi)|\varepsilon^{\frac{1}{p}-s} \quad (30)$$

C. Lemma

If $q\leq 1$ or if the compatibility conditions hold for $2+3n\geq -2+q\geq 0$, then $a_{0,q}(\xi)$ is bounded for $\xi\in[\pi,2\pi]$.

Proof.

We aim to establish the general case for any non-negative integer r through induction. Specifically, we derive the following recursive relation of the derivatives of $v^0(\xi)$.

And by using induction approch we got

$$\frac{d^r v^0(\xi)}{d\xi^r} = \sum_{\substack{l+s\leq r\\ l,s\geq 0}} c_{ls}(\sin\xi)^{2l-r+s}\frac{\partial^{l+s}u^0}{\partial x^l\partial y^s}(B_x(\xi),B_y(\xi)) + \sum_{0\leq r'\leq r-1} c_{r'}(\sin\xi)^{r'-r}\frac{d^{r'}v^0(\xi)}{d\xi^{r'}} \tag{31}$$

holds,

To bound the second term on the right-hand side of (31), We use Lemma 2.2.1

$$\frac{\partial^l u^0}{\partial x^l}(x,y) = \sum_{l'+s'\leq l-1,l',s'\geq 0} g_{l'ls'}(x)\frac{\partial^{l'+s'}f}{\partial x^{l'}\partial y^{s'}}(x,C_u(x)) + c_l\int_y^{C_u(x)}\frac{\partial^l f}{\partial x^l}(x,s)ds, \tag{32}$$

$$\left\{\frac{\partial^s}{\partial y^s}\left[\frac{\partial^l u^0}{\partial x^l}\right]\right\}(x,y) = \sum_{l'+s'\leq l-1,l',s'\geq 0} g_{l'ls's}(x)\frac{\partial^{l'+s'}f}{\partial x^{l'}\partial y^{s'}}(x,C_u(x)) + c_{ls}\left\{\frac{\partial^{s-1}}{\partial y^{s-1}}\left[\frac{\partial^l f}{\partial x^l}\right]\right\}(x,y), \tag{33}$$

where

$$\frac{\partial^{-1}f}{\partial y^{-1}}(x,y) = \int_y^{C_u(x)} f(x,s)\,ds, \quad \text{and} \quad |g_{l'ls's}(x)| \leq \kappa C_u(x)^{-(-1+2l-2l'-s')}. \tag{34}$$

Then,we rewrite

$$\begin{aligned}\frac{1}{(\sin\xi)^{q-r}}\frac{d^r v^0}{d\xi^r}(\xi) = &\sum_{\substack{l+s\leq r,l,s\geq 0\\ l'+s'\leq l-1,l',s'\geq 0}} \tilde{g}_{l'ls's}(\cos\xi)\left(\frac{\partial^{l'+s'}}{\partial x^{l'}\partial y^{s'}}f\right)(\cos\xi,\sin\xi)\\ &+\sum_{\substack{l+s\leq r,\\ l,s\geq 0}}\tilde{c}_{ls}(\sin\xi)\left(\frac{\partial^{s-1}}{\partial y^{s-1}}\left[\frac{\partial^l}{\partial x^l}f\right]\right)(\cos\xi,\sin\xi)\\ &+\sum_{0\leq r'<r-1}\frac{c_{r'}}{(\sin\xi)^{q-r'}}\frac{d^{r'}v^0(\xi)}{d\xi^{r'}},\end{aligned} \tag{35}$$

where $|\tilde{g}_{l'ls's}(\cos\xi)| \leq \kappa(\sin\xi)^{-(1-2l'-s'+q-s)}$ and $|\tilde{c}_{ls}(\sin\xi)| \leq \kappa(\sin\xi)^{-(q-2l-s)}$.

Then, since

$$0 \leq 2(p'+l') + q' + s' \leq -1 + q - s - 1 \leq -2 + q,$$

it follows that

$$\frac{\partial^{p'+q'}}{\partial x^{p'}\partial y^{q'}}\left(\frac{\partial^{l'+s'}}{\partial x^{l'}\partial y^{s'}}f\right) = 0 \quad \text{at } (\pm 1,-2) \quad \text{for } 0 \leq 2p'+q' \leq -1-2l'-s'+q-s-1. \tag{36}$$

Similarly, considering

$$0 \leq 2(p'+l') + q' + s' - 1 \leq -2 + q,$$

we deduce that

$$\frac{\partial^{p'+q'}}{\partial x^{p'}\partial y^{q'}}\left(\frac{\partial^{s-1}}{\partial y^{s-1}}\left[\frac{\partial^l}{\partial x^l}f\right]\right) = 0 \quad \text{at } (\pm 1,-2) \quad \text{for } 2p'+q' \leq q-2l-s-1. \tag{37}$$

This results in the boundedness of the first and second terms, by using Lemma 2.1. We demonstrate the boundedness of the third sum on the right-hand side of equation (35) using an inductive approach on the variable r. Consider the sum defined by

$$S_r = \sum_{0 \le r' < r-1} \frac{c_{r'}}{(\sin \xi)^{q-r'}} \frac{d^{r'} v^0(\xi)}{d\xi^{r'}},$$

where $c_{r'}$ are coefficients, ξ is the variable, and v^0 is a function of ξ. We aim to show that S_r is bounded for all $r \ge 0$. We proceed by induction on r.

Initial Step: For $r = 0$,

$$S_0 = 0,$$

as there are no terms in the sum, hence S_0 is trivially bounded.

Inductive Step: Assume S_r is bounded for $r \ge 0$.

Consider the sum defined by

$$S_{r+1} = \sum_{0 \le r' < r-1} \frac{c_{r'}}{(\sin \xi)^{q-r'}} \frac{d^{r'} v^0(\xi)}{d\xi^{r'}} + \frac{c_{r-1}}{(\sin \xi)^{q-r+1}} \frac{d^{r-1} v^0(\xi)}{d\xi^{r-1}}. \tag{38}$$

If we substitute the right-hand side of (38) with expression (35) for S_r, then under the assumption that S_r is bounded, S_{r+1} will also be bounded.

D. Lemma

If $q \le 1$ or if the compatibility conditions are satisfied for $2 + 3n \ge -2 + q \ge 0$, then the following inequality is established:

$$\left| \frac{\partial \theta^0}{\partial r} \right|_{L^2(D^*)} \le \kappa \varepsilon^{-\frac{1}{2}},$$

$$\left| \frac{\partial \theta^0}{\partial \xi} \right|_{L^2(D^*)} \le \kappa \varepsilon^{\frac{1}{2}}.$$

$$\left| L_\varepsilon (\theta^0 - \bar{\theta^0}) \right|_{L^2(D^*)} \le \kappa \varepsilon^{\frac{1}{2}}. \tag{39}$$

Proof.

Applying Lemma 2.1 with $s = 1$, $m = 0$, $l = 0$, and $n = 0$, and using Lemma 2.2 we obtain an upper bound:

$$\left| \frac{\partial \theta^0}{\partial r} \right|_{L^2(D^*)} \le \kappa \epsilon^{-1/2}.$$

Similarly, the boundedness of the derivative with respect to ξ:

$$\left| \frac{\partial \theta^0}{\partial \xi} \right|_{L^2(D^*)} \le \kappa \epsilon^{1/2}.$$

is also easily derived from Lemma 2.1. We now estimate $L_\epsilon(\theta^0 - \theta^0)$. From from Lemmas 2.2, we note that

$$\begin{aligned}
\left|\frac{\partial^2(\theta^0-\bar{\theta}^0)}{\partial\xi^2}\right|_{L^2(D^*_{R/2})} &= \left|\frac{\partial^2\theta^0}{\partial\xi^2}(\delta-R)\right|_{L^2(D^*_{R/2})} \leq \kappa\epsilon^{\frac{1}{2}},\\
\left|\frac{\partial(\theta^0-\bar{\theta}^0)}{\partial r}\right|_{L^2(D^*_{R/2})} &= \left|\frac{\partial\theta^0}{\partial r}(\delta-R)\right|_{L^2(D^*_{R/2})} + \left|\theta^0\frac{\partial(\delta-R)}{\partial r}\right|_{L^2(D^*_{R/2})} \leq \kappa\epsilon^{-\frac{1}{2}}+\kappa\epsilon^{\frac{1}{2}} \leq \kappa\epsilon^{-\frac{1}{2}},\\
\left|\frac{\partial(\theta^0-\bar{\theta}^0)}{\partial\xi}\right|_{L^2(D^*_{R/2})} &= \left|\frac{\partial\theta^0}{\partial\xi}(\delta-R)\right|_{L^2(D^*_{R/2})} \leq \kappa\epsilon^{\frac{1}{2}},\\
\left|\frac{\partial^{l+m}(\bar{\theta}^0-\theta^0)}{\partial r^l\partial\xi^m}\right|_{L^2(D^*_{R/2})} &= \left|\frac{\partial^{l+m}(\bar{\theta}^0-\theta^0)}{\partial r^l\partial\xi^m}\right|_{L^2(D^*_{R/2})} \leq \kappa\epsilon^{\frac{1}{2}(m'-l)},\\
&\text{where } m' = \begin{cases} 0, & \text{if } m=0,\\ 1, & \text{if } m=1 \text{ or } 2.\end{cases}
\end{aligned} \tag{40}$$

Using (2.6) and (2.8), we find that

$$\begin{aligned}
\left|L_\epsilon(\bar{\theta}^0-\theta^0)\right|_{L^2(D^*_{R/2})} &\leq \sum_{\substack{1\leq m+l\leq 2\\ 0\leq l\leq 1}} \left|\varepsilon S_{l,m}(r,\cos\xi,\sin\xi)\frac{\partial^{l+m}(\bar{\theta}^0-\theta^0)}{\partial r^l\partial\xi^m}\right|_{L^2(D^*_{R/2})}\\
&\quad + \left|\frac{\cos\xi}{H'(1-r)}\frac{\partial(\bar{\theta}^0-\theta^0)}{\partial\xi}\right|_{L^2(D^*_{R/2})}\\
&\leq \kappa\epsilon^{\frac{1}{2}}+\kappa\epsilon^{\frac{1}{2}} \leq \kappa\epsilon^{\frac{1}{2}}.
\end{aligned} \tag{41}$$

E. Theorem

The following estimate holds:

$$\|u^\varepsilon - u^0 - \bar{\theta}^0\|_{H^1(D)} \leq \kappa\varepsilon^{\frac{1}{2}}, \tag{42}$$

where $\bar{\theta}^0$ is the corrector in (9).

Proof.

For the error analysis of solution, writing $w = u^\varepsilon - u^0 - \bar{\theta}^0$, we deduce that

$$\begin{cases} -\varepsilon\Delta w - w_y = \text{R.H.S.},\\ w = 0 \quad \text{on} \quad \partial D. \end{cases} \tag{43}$$

Using the approximate form $\bar{\theta^0}$ for θ^0 we write $L_\varepsilon\bar{\theta^0} = L_\varepsilon\theta^0 + L_\varepsilon(\bar{\theta^0}-\theta^0)$, and then $(L_\varepsilon\theta^0,\varphi) = (L_\varepsilon\theta^0,\varphi\delta(r))$ for all $\varphi \in H_0^1(D)$ where $(,)$ is the scalar product in the space $L^2(D)$ and $\delta(r)$ is a smooth function such that $\delta(r)=1$ if $r \leq 3R/4$ and $\delta(r)=0$ if $r \geq R/2$. Note that $\theta^0 = 0$ for $r \leq R/2$.

We first observe that

$$R.H.S. = \varepsilon\Delta u^0 - L_\varepsilon(\theta^0) + L_\varepsilon(\theta^0-\bar{\theta^0}). \tag{44}$$

Taking the scalar product of (44) with $e^y w$ we find with D^*:

$$\varepsilon\|w\|^2_{H^1(D)} + \|w\|^2_{L^2(D)} \leq |\varepsilon(\Delta u^\varepsilon, e^y w\delta(r))| + \left|(L_\varepsilon(\theta^0), e^y w\delta(r))\right| + \left|(L_\varepsilon(\theta^0 - \bar{\theta^0}), e^y w\delta(r))\right| \tag{45}$$

$$\begin{aligned}
&\leq \kappa\varepsilon\|u^0\|_{H^1(D)}\|w\|_{H^1(D)} \\
&\quad + \left|\left(-\varepsilon \sum_{\substack{1\leq m+l\leq 2 \\ 0\leq l\leq 1}} S_{l,m}(r,\cos\xi,\sin\xi)\frac{\partial^{l+m}\theta^0}{\partial r^l \partial\xi^m} - \frac{\cos\xi}{H'(1-r)}\frac{\partial\theta^0}{\partial\xi}, e^y w\delta(r)\right)\right| \\
&\quad + \left|(L_\varepsilon(\theta^0 - \bar{\theta^0}), e^y w\delta(r))\right| \qquad (46) \\
&\leq \kappa\varepsilon\|u^0\|_{H^1(D)}\|w\|_{H^1(D)} \\
&\quad + \varepsilon(\kappa\|S_{0,1}\|_{L^2(D^*)} + \kappa\|S_{0,2}\|_{L^2(D^*)})\left\|\frac{\partial\theta^0}{\partial\xi}\right\|_{L^2(D^*)}\left(\left\|\frac{\partial w}{\partial\xi}\delta(r)\right\|_{L^2(D^*)} + \|w\delta(r)\|_{L^2(D^*)}\right) \\
&\quad + \left(\kappa\left\|\varepsilon S_{1,0}\frac{\partial\theta^0}{\partial r} + \varepsilon S_{1,1}\frac{\partial^2\theta^0}{\partial r\partial\xi}\right\|_{L^2(D^*)} + \kappa\left\|\cos\xi\frac{\partial\theta^0}{\partial\xi}\right\|_{L^2(D^*)}\right)\|w\delta(r)\|_{L^2(D^*)} \\
&\quad + \kappa\left\|L_\varepsilon(\theta^0 - \bar{\theta^0})\right\|_{L^2(D^*_{R/2})}\|w\delta(r)\|_{L^2(D^*)}. \qquad (47)
\end{aligned}$$

Using Lemma 2.2, we obtain

$$\|w\|_{L^2(D)} + \varepsilon^{\frac{1}{2}}\|w\|_{H^1(D)} \leq k\varepsilon^{\frac{1}{2}}. \tag{48}$$

We now establish the semi-analytic SL-PINN method as

$$\widetilde{v}(r,\xi;\boldsymbol{\theta}) = \left(\hat{v}(r,\xi;\boldsymbol{\theta}) - \hat{v}(1,\xi;\boldsymbol{\theta})\bar{\varphi}^0\right)C(r,\xi) \tag{49}$$

where $C(r,\xi)$ is given by

$$C(r,\xi) = \begin{cases} 1 - r^3, \text{ if } 0 \leq \xi \leq \pi, \\ 1 - r^3 - (r\sin\xi)^3, \text{ if } \pi < \xi < 2\pi, \end{cases} \tag{50}$$